

**Osteochondral Repair by a Novel Interconnecting Collagen–Hydroxyapatite Substitute:
A Large-Animal Study**

Corrado Sosio, MD,^{1,*} Alessia Di Giancamillo, DVM, PhD,^{1,*} Daniela Deponti, PhD,¹
Francesca Gervaso, PhD,² Francesca Scalera, PhD,² Marco Melato, MD,³ Marino Campagnol, DVM,
PhD,⁴ Federica Boschetti, PhD,^{1,5} Alessandro Nonis, MS,⁶ Cinzia Domeneghini, DVM,⁷
Alessandro Sannino, PhD,² and Giuseppe Michele Peretti, MD^{1,8}

¹IRCCS Istituto Ortopedico Galeazzi, Milan, Italy.

²Department of Engineering for Innovation, University of Salento, Lecce, Italy.

³Residency Program in Orthopaedics and Traumatology, Università degli Studi di Milano,
University of Milan, Milan, Italy.

⁴CRABCC, Rivolta d'Adda (CR), University of Milan, Milan, Italy.

⁵Laboratory of Biological Structure Mechanics, Department of Structural Engineering Politecnico di
Milano, Milan, Italy.

⁶University Center for Statistics in the Biomedical Sciences (CUSSB), Vita-Salute San Raffaele
University, Milan, Italy.

Departments of ⁷Health, Animal Science and Food Safety and ⁸Biomedical Sciences for Health, Università
degli Studi di Milano, University of Milan, Milan, Italy.

*These authors have equally contributed to the completion of this work.

Abstract

A novel three-dimensional bicomponent substitute made of collagen type I and hydroxyapatite was tested for the repair of osteochondral lesions in a swine model. This scaffold was assembled by a newly developed method that guarantees the strict integration between the organic and the inorganic parts, mimicking the biological tissue between the chondral and the osseous phase. Thirty-six osteochondral lesions were created in the trochlea of six pigs; in each pig, two lesions were treated with scaffolds seeded with autologous chondrocytes (cell + group), two lesions were treated with unseeded scaffolds (cell - group), and the two remaining lesions were left untreated (untreated group). After 3 months, the animals were sacrificed and the newly formed tissue was analyzed to evaluate the degree of maturation. The International Cartilage Repair Society (ICRS) macroscopic assessment showed significantly higher scores in the cell - and untreated groups when compared with the cell + group. Histological evaluation showed the presence of repaired tissue, with fibroblast-like and hyaline-like areas in all groups; however, with respect to the other groups, the cell - group showed significantly higher values in the ICRS II histological scores for “cell morphology” and for the “surface/superficial assessment.” While the scaffold seeded with autologous chondrocytes promoted the formation of a reparative tissue with high cellularity but low glycosaminoglycans (GAG) production, on the contrary, the reparative tissue observed with the unseeded scaffold presented lower cellularity but higher and uniform GAG distribution. Finally, in the lesions treated with scaffolds, the immunohistochemical analysis showed the presence of collagen type II in the peripheral part of the defect, indicating tissue maturation due to the migration of local cells from the surroundings. This study showed that the novel osteochondral scaffold was easy to handle for surgical implantation and was stable within the site of lesion; at the end of the experimental time, all implants were well integrated with the surrounding tissue and no signs of synovitis were observed. The quality of the reparative tissue seemed to be superior for the lesions treated with the unseeded scaffolds, indicating the promising potential of this novel biomaterial for use in a one-stage procedure for osteochondral repair.

Introduction

Articular cartilage and subchondral bone form a well-integrated system, with unique biomechanical properties, which provides the efficient transmission of high acting loads.^{1,2} This osteochondral core is

frequently damaged by trauma and disease; as a consequence, the joint undergoes an osteoarthritis degeneration³⁻⁵ leading to severe pain, joint deformity, and loss of joint motion.^{6,7} The degeneration of the osteochondral tissue may initiate at different locations. It could start from the subchondral bone, which becomes weaker and unable to support proper loading, causing cartilage degeneration.⁸ On the other hand, the lesion may begin in the cartilage tissue, therefore inducing altered stimulus to the subchondral bone, which becomes sclerotic.⁹ Both scenarios may be responsible for modifying the performance of the osteochondral core.

As the osteochondral tissue has a poor spontaneous regenerative potential, its treatment represents a major challenge in the orthopedic field. In the clinical practice, several solutions have been proposed for repairing these lesions, of which the most commonly utilized are those based on the potential of the cells recruited from the bone marrow to differentiate into chondrocytes. However, fibrous tissue and fibrocartilage represent the predominant repairing tissues derived from these procedures and these tissue types do not exhibit the mechanical properties of native hyaline cartilage.¹⁰ To tackle this problem, osteochondral transplantation has been widely used as autologous tissue^{11,12} and as allograft.^{13,14} However, the autologous procedures are strongly limited by the donor-site morbidity and by the difficulty of carving the surface of the tissue transplant into the correct shape.¹⁵ On the other hand, the allograft procedures may be influenced by higher costs, tissue availability, risk of disease transmission, and issues regarding mechanical stability and cell vitality.¹³ In the recent years, the application of the tissue engineering approaches for repairing osteochondral defects has received an increasing interest. However, because of the extremely differing natures of cartilage and bone when a monophasic scaffold is used, the natural environment is not well duplicated and the new tissue is not properly formed.^{16,17} Consequently, modern approaches focus on the design and development of heterogeneous scaffolds obtained by the combination of different layers corresponding to the cartilage and bone regions. In the literature, several bilayered scaffolds are described with the superficial part modeling the cartilage (usually made of collagen) and the deeper layer modeling the subchondral bone (usually made of different materials, including hydroxyapatite [HA]).¹⁸⁻²⁰ Some studies have reported results on bilayered materials in which as an alternative to collagen, chitosan,²¹ poly(lactide-co-glycolide),²² or polyvinyl alcohol (PVA)²³ were used for the cartilaginous part.

In our study, a novel three-dimensional collagen/HA osteochondral substitute is proposed, surrounded in circumference by a thin layer of collagen, and characterized by a stable preintegration between the osteo and chondral components, easy surgical handling, and compliant at the implant site. The aim of this study was to evaluate the potential of this bicomponent substitute for repairing osteochondral lesions in a swine model. In particular, the lesions were treated with the chondral part of the substitute seeded with autologous chondrocytes or in a cell-free formulation and the reparative tissues were compared to that of untreated lesions to evaluate the capacity of the substitute to induce restoration of the osteochondral core.

Materials and Methods

Osteochondral substitute fabrication

A novel three-dimensional bicomponent substitute was developed. The two components, which were characterized separately in previous studies,^{24–26} consist of a superficial part made of collagen, which partially penetrates into a HA sponge. To obtain a partial but strong interconnection between the collagen and HA part, a multistep procedure was developed, which is described below (Fig. 1).

Fabrication of the porous HA cylinders with appropriate dimensions. HA macrochanneled porous scaffolds were produced by a polymeric sponge templating method using a reactive submicron powder synthesized by hydroxide precipitation sol–gel route. The HA powder was calcined in air at 900°C for 60 min before use. The porous HA scaffolds were obtained by impregnating small cylinders (diameter = 9.7 mm, height = 8.6 mm) of a polyurethane sponge (density of 30 kg/m³, 25 ppi, kindly provided by ORSA Foam S.P.A.) with the slurry that was prepared by adding the HA powder (70 wt%) within a 2 wt% PVA solution. Dolapix CE-64 (Zschimmer & Schwarz) was used as a dispersant to obtain the optimal slurry viscosity for the impregnation. The infiltrated sponges were then gently squeezed to remove the excess slurry, dried for 24 h in air, heat treated at 500°C to burnout the sponges, and finally sintered at 1300°C. The polyurethane sponge dimensions were slightly bigger than those of the final desired biphasic substitutes to compensate for sintering shrinkage.

1. Fabrication through stereolithography of a mold (mold A). The mold shape and dimensions were properly designed to sustain the HA scaffold and, simultaneously, to allow for the lyophilization of the collagen

slurry. An interconnection zone was obtained, where the two materials were copresent for a pre-established distance (1 mm) (Fig. 2A, black arrows).

2. Lyophilization and crosslinking of the collagen scaffolds inside the mold A. The collagen segment was formed using a freeze-drying technique: briefly, freeze-dried membranes of type I equine collagen (Antema®; kindly provided by Opocrin S.P.A.) were pulverized in a refrigerated mill and the obtained collagen flakes were suspended in double-distilled water to obtain a collagen concentration of 2 wt%. The slurry was agitated by a magnetic stirrer for 2 h and poured into the mold A. The HA scaffolds from step 1 were then inserted in the mold, which was partially filled by collagen slurry. The samples were frozen using a cooling rate of $-1^{\circ}\text{C}/\text{min}$, reaching -40°C , then freeze-dried (Lyo 1). A dehydrothermal (DHT) crosslinking treatment was applied to the samples.
3. Fabrication through stereolithography of a mold (mold B). The mold B was designed with the aim of making a perfectly cylindrical substitute with the final desired dimensions, surrounded by a very thin layer of collagen (Fig. 2B). This collagen layer had the double effect of eliminating the small indentation derived from the use of the mold A and facilitating the insertion in the osteochondral lesion at the moment of implantation surgery. For this reason, the final diameter of the mold B was slightly superior to that of the mold A.
4. Lyophilization and crosslinking of the collagen scaffolds inside the mold B. The biphasic substitutes were inserted in the mold B and then covered all around by collagen slurry. The samples were frozen using a cooling rate of $-1^{\circ}\text{C}/\text{min}$, reaching -40°C , and again freeze-dried (Lyo 2). A DHT crosslinking treatment was applied to the samples.
5. The obtained substitutes were sterilized in an oven under vacuum at 160°C for 2 h.

Chondrocyte isolation, expansion, and seeding

Six 4-month-old Large White pigs (60 kg – 4 kg of body weight) were used for this study. All animals were treated in accordance with both policies and principles of laboratory animal care, approved by the Italian Ministry of Health (D.Lgs 116/92, transposition of the directive 86/609/EU) and in compliance with the Directive 2010/63/EU. Pigs were housed in groups in standard boxes in temperature-controlled rooms ($15\text{--}20^{\circ}\text{C}$) and were allowed free mobilization; they underwent an adaptation and observation

period for 1 week before surgery and fed twice daily with a standard commercial pig diet. Before the experiments, the pigs were fasted overnight but given free access to water. For all procedures, heavy sedation was obtained in 10 min by ketamine 10 mg/kg (Lobotor; Acme Srl Italia) and midazolam 0.5 mg/kg (Midazolam PHG; Hospira Italia Srl) intramuscularly. Anesthesia was obtained by an oronasal mask with a mixture of isoflurane 4% and oxygen and maintained through intubation with the same gas mixture (isoflurane 2–2.5%). Pre-emptive analgesia was provided with ketorolac (Toradol; InnovaPharma SpA) 1 mg/kg IV at the moment of intubation and intraoperative analgesia with lidocaine (Lidocaina 2%; Fort Dodge Animal Health Spa) 2 mg/kg IV and 0.2 mg/kg/h. The animals received enrofloxacin (Baytrril Soluz Iniet 5%; Bayer SpA Div. Sanità Animale) 5 mg/kg IV and cefotaxime (Cefotaxime Hosp; Hospira Italia Srl) 1 g IV at the time of surgery and amoxicillin long acting (Clamoxyl La; Pfizer Italia Srl Div. Vet.) 15 mg/kg/48h for the following 10 days. Postoperative analgesia was provided with meloxicam (Me-tacam Iniet; Boehringer Ingelheim Div. Vet.) 0.4 mg/kg/12h/ 10 days. The animals were placed in the supine position. A longitudinal paramedian incision was made in the medial aspect of the right knee. The vastus medialis muscle, which completely surrounds the patella in the pig, was sectioned to expose the articular capsule. A capsulotomy was performed and the patella was dislocated laterally to expose the articular surface of the trochlear groove.²⁷ Six cartilage lesions measuring 6 mm in diameter and extending up to the border with the calcified cartilage were produced in the patellar groove with a standardized core punch (Fig. 3A). The chondral plugs were placed in 50-mL test tubes containing phosphate-buffered saline (PBS) and the antibiotic/antimycotic solution. The wound was then closed in layers in a standard manner. An impermeable dressing was applied. No immobilization was applied after operation and the animal was allowed to move freely.

Cartilage slices were obtained from chondral plugs and were digested in Ham's medium (Celbio) containing 0.1% collagenase type 2 (DBA-Italia Srl) and 1% of the antibiotic/antimycotic solution (10,000 U penicillin, 10 mg streptomycin, and 25 mg Amphotericin B/mL in 0.9% sodium chloride; Sigma Chemical Co.). The specimens were incubated over-night in an oscillating water bath at 37°C.

Undigested tissue and debris were removed by filtering the cell suspension using a 100-mm sterile filter (BD Falcon). The cell suspension obtained was centrifuged at 1400 rpm for 10 min. The cell pellet was washed twice in PBS (Celbio) and 2% antibiotic/antimycotic solution. Viability of the chondrocytes

was assessed by Trypan blue staining (Sigma) and recorded as a percentage of viable chondrocytes per high-power field. The exact cell count per milliliter was established using a hemocytometer. Only those chondrocyte-cultures having a viability score of 90% or greater were used. Fresh chondrocytes were plated at a concentration of $10,000 \text{ cells/cm}^2$ and cultured in DMEM (Lonza) containing 10% fetal bovine serum (FBS; Euroclone), 1% glutamine (EuroClone), and 1% antibiotic/ antimycotic solution (Sigma), 5 ng/mL fibroblast growth factor-2 (FGF-2; R&D Systems), and 10 ng/mL transforming growth factor beta 1 (TGFb-1) (R&D Systems); the medium was changed thrice a week. After two passages, the dedifferentiated chondrocytes were collected, resuspended in a solution containing bovine fibrinogen (Fluka Chemie GmbH), aprotinin (Sigma), and tranexamic acid (Sigma), and adjusted to a concentration of $80 \cdot 10^6 \text{ cells/mL}$. Then, 100 mL of the fibrinogen/cell suspension was seeded onto the collagen sponges ($8 \cdot 10^6 \text{ cells/scaffold}$) prepared according to the design parameters optimized previously. After complete cell absorption, 100 mL of thrombin (1.37 mg/mL; Chemicon International, Inc.) was added to form fibrin glue.^{28–33} After 30 min, complete polymerization was reached and the scaffolds were placed in culture flasks for the *in vitro* culture. The seeded scaffolds were cultured *in vitro* for 3 weeks in DMEM (Lonza) containing 10% FBS (Euroclone), 1% glutamine (EuroClone), and 1% antibiotic/antimycotic solution (Sigma), ascorbic acid 50 mg/mL (Sigma), and 10 ng/mL transforming growth factor beta 3 (TGFb-3) (R&D Systems); the medium was changed thrice a week (Fig. 3B).

Study design

Animals (70 kg of body weight at this point) were anesthetized (as previously described) and placed in the supine position. A longitudinal paramedian incision was made in the medial aspect of the right knee on the previous skin scar, duplicating the prior surgical approach. The articular capsule was open and the previous sites of cartilage harvest were identified. The repairing tissue formed in the six previous chondral lesions was removed and six new osteochondral lesions encircling the previous defect areas were performed with a standardized core punch measuring 8 mm in diameter and 9 mm in depth. The lesions resulted well contained and surrounded by healthy cartilage tissue. Two collagen/HA substitutes seeded with autologous chondrocytes (cell + group) and two unseeded collagen/HA substitutes (cell - group) were implanted in each pig; two lesions per animal were left without any implant (untreated group) (Fig. 3C). Care

was taken in rotating the treatment to all six experimental lesion sites (proximal, intermediate, and distal on the medial and lateral aspects of the patellar groove). The capsule was then carefully closed to maintain the anatomical patellar tracking and the wound was sutured in layers. Postoperative care, medications, and dressings were as previously described. The animals were able to stand on the operated leg and allowed to walk freely. Generally, all animals were able to stand and bear full weight on four legs after 24–72 h postoperatively. Twelve weeks after implantation, all animals (90 kg of body weight at this point) were euthanized under deep anesthesia with an intravenous injection of KCl, the knee joints opened, and the repaired tissue removed and evaluated as described below.

Tissue repair evaluation

Gross evaluation. The macroscopic assessment of the re-paired tissue was evaluated using the International Cartilage Repair Society (ICRS) macroscopic score, which considers the degree of defect repair, the integration to the border zone, and the macroscopic appearance. Two observers, both blind to the treatment, independently scored the specimens.

Histochemical analysis. The repaired tissue was removed together with the surrounding healthy tissue. Each sample was cut in half, along the central axis of the lesions: half the sample was used for histochemical analysis and the other half for biochemical analysis. The samples processed for histochemistry were fixed in 10% (v/v) phosphate-buffered formaldehyde, then dehydrated in a graded 50% (v/v), 70% (v/v), 95% (v/v), and 100% (v/v) ethanol series, embedded in paraffin, and cut into 4-mm-thick sections. Finally, the sections were stained with Safranin O, using a standard staining protocol, for the evaluation of the morphology and glycosaminoglycans (GAG) deposition. The experimental samples were analyzed at the optical microscope to evaluate the histological parameters established by ICRS II; each criterion was evaluated based on the visual analog scale and graded from 0 to 100.³⁴ Some sections were used for immunohistochemical analysis of collagen type I and II (Chondrex staining kit; Chondrex, Inc.). After rehydration, heat-induced antigen retrieval was performed by treating these sections in citrate buffer, pH 6.0, in a microwave oven; sections were then washed thrice in PBS (pH 7.4). Before immunostaining, sections were treated in a 2% hyaluronidase solution (Sigma) at room temperature for 30

min. To block the endogenous peroxidase activity, sections were incubated in an aqueous solution of 1% H_2O_2 for 30 min at room temperature and then washed thrice in PBS. Sections were incubated overnight with the mouse anti-collagen type II and type I antibody (Chondrex, Inc.; 1:500). A labeled biotin secondary antibody streptavidin peroxidase (1:500) was applied for 1 h at room temperature. The peroxidase activity was visualized with diaminobenzidine (DakoCytomation) and H_2O_2 as substrates. All incubations were performed in a moist chamber at room temperature, using PBS for washes between incubation steps. Sections were counterstained with hematoxylin, dehydrated, and mounted in a mounting medium. Photomicrographs were taken with an Olympus BX51 microscope (Olympus) equipped with a digital camera and final magnifications were calculated.

Biochemical analyses. The biochemical analysis was performed on the other half of samples for each experimental condition (cell + group, cell - group and untreated group). Some native cartilage slices were previously harvested from the contralateral knees and were frozen as a control tissue for biochemical analysis. The samples were digested in papain (Sigma) for 16–24 h at 60°C ; the digestion solution was composed of 125 mg/mL of papain (Sigma) in 100 mM sodium phosphate, 10 mM sodium EDTA (Sigma), 10 mM cysteine hydrochloride (Sigma), 5 mM EDTA adjusted to pH 6.5 and brought to 100 mL of solution with distilled water. After the digestion, the samples were stored at -80°C until analysis. Aliquots of the digested samples were assayed separately for proteoglycan and DNA contents. Proteoglycan content was estimated by quantifying the amount of sulphated glycosaminoglycans using the 1,9-dimethylmethylene blue dye binding assay (Polysciences, Inc.) and a microplate reader (wavelength: 540 nm). The standard curve for the analysis was generated by using bovine trachea chondroitin sulphate A (Sigma). DNA content was evaluated with the Quant-iT Picogreen dsDNA Assay Kit (Molecular Probes, Invitrogen) and a fluorescence microplate reader and standard fluorescein wavelengths (excitation 485 nm, emission 538 nm, cut-off 530 nm). The standard curve for the analysis was generated using the bacteriophage lambda DNA supplied with the kit.

Biomechanical analyses. The mechanical properties of the repaired tissue were evaluated by the microindentation test. In particular, biomechanical tests were performed both on samples harvested from

the experimental animals and on samples of swine articular cartilage obtained from a normal femoral condyle, to evaluate the mechanical behavior of the repaired tissue and to compare it with the properties of native articular cartilage. The microindentation test was performed by an electromagnetic machine (Enduratec ELF 3200; Bose Corporation, ElectroForce Systems Group), equipped with a 22 N load cell. Indentation creep testing of all samples was performed using plane-ended indenters with a diameter of 2.0 mm. In order to maintain hydration, samples were kept in a PBS bath throughout all the tests. A preload of - 0.01 N was applied, then each specimen was mechanically tested under creep stepwise micro-indentation tests applying two increasing levels of force (- 0.02 and - 0.04 N) at a compression rate of 0.1 N/s for 1220 and 1620 s, respectively. Indenter displacement was finally evaluated. Mechanical properties were evaluated using the mathematical formulation proposed by Hayes *et al.* that models cartilage as a mono-phasic material bonded to a rigid space.³⁵

Statistical analysis. Descriptive statistics were used to determine groups' means and standard deviations for numerical data, and comparisons were performed using analysis of variance and Kruskal–Wallis test. Statistical significance was defined as a *p*-value of < 0.05.

Results

Morphology and scoring of the repair tissue

At the opening of the joint, all grafts were still in their original location and were stable in the site of implant. The repair tissue was well integrated to the surrounding tissue and no signs of synovitis were revealed. The macroscopic assessment, evaluated by the ICRS macroscopic score, showed a lower score for the cell + group when compared with the cell - and untreated group (ANOVA, $p = 0.003$) (Fig. 4). Histological evaluation showed the presence of a newly formed repair tissue, with areas of fibrotic-like appearance and areas of hyaline-like features in all groups. The three different experimental groups showed statistically significant differences in scores only in two parameters, as established by the ICRS II histological scale; in particular, the cell - group showed higher scores for cell morphology and for the surface/superficial assessment, with respect to the cell + group and untreated group (Kruskal–Wallis, $p = 0.021$ and $p = 0.002$, respectively) (Fig. 5). The histological staining with Safranin O showed that the cell - group was

characterized by a linear superficial layer with a uniform GAG distribution throughout the lesion site (Fig. 6B, arrows); moreover, the cells were oval (chondrocyte like) and some of them were surrounded by lacunae (Fig. 6E, arrows). The cell + group and the untreated group showed irregular superficial layers with hollows (Fig. 6A, C, asterisk) and the cell morphology was mainly fibroblast like with no lacunae (Fig. 6D, F, arrows). In all groups, the reparative tissue appeared to be well integrated with the native cartilage (Fig. 6G–I, lines). A reorganization of the subchondral bone was evident although it was not completely recovered at this early time point. Immunohistochemical analysis showed in the un-treated group a scarce immunoreactivity for collagen type II and type I (Figs. 7A and 8A), while in the scaffold groups, a light immunopositivity was present in the central defect area and a strong reactivity in the peripheral part (Figs. 7B, C and 8B, C arrows), especially for type II collagen.

Biochemical analysis of the repaired lesions

The biochemical analysis showed that, with respect to native cartilage, only the cell + group showed a higher cellularity, while the GAG production and GAG/DNA ratio were lower in all groups (Dunnett test, $p < 0.01$) (Fig. 9A). Comparing only the experimental samples, the cell + group showed a higher cellularity in comparison to the others, while the GAG/DNA ratio was higher in the untreated group with respect to the cell + and cell - group (ANOVA, $p < 0.01$); no differences were observed in the GAG production among the different experimental groups (Fig. 9B).

Biomechanical analysis

Figure 10 resumed the Young's modulus values obtained from the microindentation tests. The biomechanical analysis showed significantly higher Young's modulus values for native cartilage with respect to the experimental groups (Mann–Whitney, $p < 0.05$), while no significant differences were revealed between the three experimental groups.

Discussion

This study demonstrates the potential of a novel three-dimensional bicomponent substitute made of an organic/inorganic material (collagen-HA) for the repair of osteochondral lesions in the preclinical large-

animal setting. In particular, the unseeded scaffold showed higher scores for the cell morphology and the surface/superficial assessment parameters compared to the untreated lesions (natural repair) and to the lesions treated with scaffolds seeded, in the chondral aspect of the composite, with expanded autologous chondrocytes.

The substitute was made of a superficial collagen type I scaffold, which partially extended into an underlying HA sponge. The chondral component was previously characterized and tested for its capacity to support cartilage tissue engineering, was found to allow for a homogeneous distribution of the cells following seeding, and facilitate a cartilaginous differentiation *in vivo* or *in vitro* under proper chondrogenic stimuli.^{32,33} The composite was successfully produced by means of the fabrication of a properly designed mold through stereolithography that allowed for the obtaining of an interconnection zone where the two materials (collagen and HA) were copresent for a pre-established thickness (Fig. 1). This particular structure has the advantage of allowing for a strong integration of the two materials, and by mimicking the native tissues, of creating the ideal substratum for a proper re-population following *in vivo* implantation. Additionally, a second novelty was introduced: the presence of a thin layer of collagen material around the cylindrically shaped composite. This was obtained through the fabrication by means of stereolithography of a second mold and the subsequent lyophilization of the collagen. This feature has the dual aim of both further improving the collagen/HA integration and also facilitating the insertion of the substitute into the osteochondral lesion ensuring its ultimate stability at the moment of the implantation surgery. This second aspect was achieved by the ability to increase the diameter of the cylinder, to a certain degree, through physiological hydration, thus improving the stability following press-fit fixation without the need of additional materials, such as fibrin glue.³⁶

Osteochondral defects created in the trochlea of young pigs were treated by implanting the bicomponent scaffolds, which were either seeded with autologous chondrocytes or left unseeded. As a control, some lesions were left untreated. The use of collagen type I sponges for cartilage repair has been already adopted by several groups^{37–40} demonstrating that they can support chondrocyte survival and extracellular matrix (ECM) synthesis, leading to the maturation of the scaffold into a chondral substitute. Because one of the crucial considerations is the level of *in vitro* maturation of the engineered tissue before implantation, some authors have introduced the combination of fibrin glue to enhance scaffold seeding and *in vitro*

maturation.^{41–43} Additionally, a work recently published has specifically evaluated the effect of the timing of *in vitro* maturation of engineered cartilaginous samples embedded in fibrin glue on the tissue quality after *in vivo* implantation.³² With respect to the boneside of the defect, a HA scaffold was adopted as a bone substitute. This component was left unseeded, counting on the capacity of the mesenchymal stem cells to migrate from the adjacent bone marrow into the scaffold and to undergo an appropriate osteogenic/chondrogenic differentiation. This particular strategy represents the basis of several tissue engineering approaches utilized in clinical practice for chondral and osteochondral repair.^{44–46}

Our study provided interesting data on the ongoing osteochondral repair at 3 months postimplantation. In particular, the ICRS macroscopic assessment showed significantly higher scores in the lesions treated with the unseeded scaffold or left untreated compared to those treated with the scaffold seeded with autologous chondrocytes. Moreover, the histological evaluation showed that the repair induced by the unseeded scaffold was superior to that obtained in the other groups, thus demonstrating that the scaffold itself allowed for an early colonization and maturation of the cells derived from the local environment. In particular, two histologic parameters showed significantly higher scores in the unseeded scaffold: the morphology of the cells and the appearance of the superficial layer. While the scaffold seeded with autologous chondrocytes promoted the formation of a reparative tissue with high cellularity but low GAG production (suggesting a low chondrocyte activity), the unseeded scaffold showed a lower cellularity, but with the cells having a more chondrocyte-like phenotype (with some surrounded by lacunae). Moreover, the unseeded scaffold showed a regular superficial layer with a uniform GAG distribution throughout the lesion site. Additionally, a partial reconstruction of the subchondral bone was seen in all groups with bone forming according to the reparative osteogenesis process, which confirms the earliness of this study for the evaluation of subchondral bone structure. Finally, immunohistochemical analysis showed a stronger positive staining for collagen type II in the peripheral area of the defect for both scaffold groups, providing further evidence that cells from the surrounding tissue were able to enter the unseeded scaffold and synthesize the cartilage-like ECM. These data confirm the capacity of the scaffold to recruit undifferentiated stem cells from the bone marrow and to direct them toward a chondrogenic pathway, inducing a restoration of the defect site to a cartilaginous/ fibrocartilaginous tissue. Nonetheless, at the experimental time tested here, the quantity and the quality of the repaired tissue were far from those of

the native cartilage in both treatment groups. The biochemical and biomechanical analysis confirmed this finding, as GAG production and the Young's modulus values were lower in all experimental groups compared with those of the native tissue. Unexpectedly, the autologous chondrocytes seeded into the scaffold did not seem to provide, at this early repair time, evident advantages over the use of a scaffold alone. The rationale of using this experimental setup and these experimental time points derived from previous studies performed both *in vitro*³³ and in heterotopic *in vivo* models³² identified the ideal culture time before implantation as being 3 weeks. However, it is not known if the transplanted chondrocytes survived in this orthotopic model as the cells were not labeled. Considering the substantial changes that occur from the *in vitro* to *in vivo* environment, it is probable that other factors may have, in fact, influenced the survival and the activity of the transplanted cells, like the limited diffusion of nutrients or, more likely, the inflammatory stimuli generated within the joint cavity, which may have damaged the transplanted cells.⁴⁷⁻⁴⁹ In this hypothetical situation, tissue regeneration would depend on the activity of cells recruited into the scaffold from the lesion site. If this was the case, the fibrin glue may have represented an obstacle for the migration of these cells or for the production of the cartilaginous ECM. This could explain the higher scores recorded for the unseeded scaffold, which was assembled without fibrin glue, similarly to that reported by other researchers using polymer gels within the bone substitute.⁵⁰ In this regard, different strategies could therefore be devised for increasing the survival of the cells within a fibrin glue or any other gel or scaffold materials. On the other hand, we believe that there is still some room for improvement of cell-free scaffolds such as by the use of materials with different porosity or composition or by delivering biological stimuli from within the scaffold or administered separately.⁵¹⁻⁵⁴ Another important question is the effectiveness of the current approach in repairing large defects, as could be encountered in the clinical setting. In this situation, a larger number of cells could be needed for seeding scaffolds of larger dimensions and therefore probably the use of stimulating factors would be desirable for maintaining the survival and secretory activity of the transplanted cells. On the other hand, in a cell-free approach, the recruitment of the reparative cells from the periphery should be guaranteed throughout the entire scaffold and would probably require a material that is both more hydrophilic and with a higher capacity for attracting and hosting the resident cells. In light of the results obtained, the main limitations of this study include the low number of animals and the short experimental time frame. A

larger number of pigs would have led to a more robust statistical analysis for the histological grading. To enlarge the number of experimental samples, six lesions per animal were produced. The different positions of the implants in the animal trochlea could have influenced the quality of the repaired tissue; however, the rotation of the sites of the different treatment groups (proximal, intermediate, and distal on the medial and lateral aspects of the patellar groove) was done to avoid this bias.²⁷ In this regard, the choice of the trochlea as a site for the lesions, compared to the more common femoral condyles, was also justified by the different range of motion of the knee in pigs, which does not reach the full extension, in comparison with humans, thus rendering this joint surface more subject to compressive loads during normal cage activity.^{55,56} The short experimental time did not allow for the evaluation of the repair process at the final stage; however, the analysis of the tissue at an early stage is critical for understanding the pathway of the repair and the phases of the maturation of the tissue. Moreover, the quantity and the quality of the ongoing repair tissue are clinically relevant aspects for the timing of joint mobilization and loading. Finally, the short follow-up has rendered negligible the animal growth during the experimental time (from 70 to 90 kg during the implant time), as the main increase of this body weight was due to the muscle mass increase and not to the skeletal growth.

In conclusion, this study showed that the novel osteochondral scaffold is easy to handle for surgical grafting and stable in the implant site; at the end of the experimental time, no signs of synovitis were revealed and all implants were well integrated to the surrounding tissue. At the early stage chosen in this study, the quality of the repaired tissue produced within the bulk of the unseeded composite scaffold demonstrated the potential of this material for a one-step procedure for osteochondral repair and justifies the effort for the further improvement of the biphasic scaffold and eventual additional orthotopic tests with a longer follow-up.

Acknowledgments

This work was funded by the Fondazione CARIPLO (project No. 5682). The authors acknowledge Dr. Alessandro Addis, Dr. Alessandro Pozzi, and Dr. Rosa Ballis for the animal care and management and for their precious help in the sample preparation and shipping. The authors thank Dr. Frascini for his support in the present study. The authors also acknowledge Rahmat Cholas for revising the English language of

this manuscript. Special thanks is given to Prof. Clelia Di Serio for the supervision of the statistical analysis and to Dr. Sanosh Kunjalukkal Padmanabhan and Dr. Antonio Licciulli for the synthesis of the HA component.

Disclosure Statement

No competing financial interests exist.

References

1. Pan, J., Zhou, X., Li, W., Novotny, J.E., Doty, S.B., and Wang, L. *In situ* measurement of transport between sub- chondral bone and articular cartilage. *J Orthop Res* 27, 1347, 2009.
2. Madry, H., van Dijk, C.N., and Mueller-Gerbl, M. The basic science of the subchondral bone. *Knee Surg Sports Traumatol Arthrosc* 18, 419, 2010.
3. Pape, D., Filardo, G., Kon, E., van Dijk, C.N., and Madry, H. Disease-specific clinical problems associated with the subchondral bone. *Knee Surg Sports Traumatol Arthrosc* 18, 448, 2010.
4. Lories, R.J., and Luyten, F.P. The bone-cartilage unit in osteoarthritis. *Nat Rev Rheumatol* 7, 43, 2011.
5. Ding, M. Microarchitectural adaptations in aging and oste-oarthritic subchondral bone issues. *Acta Orthop Suppl* 81, 1, 2010.
6. Bijlsma, J.W., Berenbaum, F., and Lafeber, F.P. Osteoarthritis: an update with relevance for clinical practice. *Lancet* 377, 2115, 2011.
7. Sellam, J., and Berenbaum, F. The role of synovitis in pathophysiology and clinical symptoms of osteoarthritis. *Nat Rev Rheumatol* 6, 625, 2010.
8. Intema, F., Hazewinkel, H.A., Gouwens, D., Bijlsma, J.W., Weinans, H., Lafeber, F.P., and Mastbergen, S.C. In early OA, thinning of the subchondral plate is directly related to cartilage damage: results from a canine ACLT-menisectomy model. *Osteoarthritis Cartilage* 18, 691, 2010.
9. Siebelt, M., Groen, H.C., Koelewijn, S.J., de Blois, E., Sandker, M., Waarsing, J.H., Müller, C., van Osch, G.J., de Jong, M., and Weinans, H. Increased physical activity severely induces osteoarthritic changes in knee joints with papain induced sulphate-glycosaminoglycan depleted

- cartilage. *Arthritis Res Ther* 16, R32, 2014.
10. Hunziker, E.B. Articular cartilage repair: basic science and clinical progress. A review of the current status and prospects. *Osteoarthritis and Cartilage* 10, 432, 2001.
 11. Hangody, L., and Füles, P. Autologous osteochondral mosaicplasty for the treatment of full-thickness defects of weight-bearing joints: ten years of experimental and clinical experience. *J Bone Joint Surg Am* 85-A Suppl 2, 25, 2003.
 12. Filardo, G., Kon, E., Perdisa, F., Balboni, F., and Marcacci, M. Autologous osteochondral transplantation for the treatment of knee lesions results and limitations at two years' follow-up. *Int Orthop* 38, 1905, 2014.
 13. Gross, A.E., Kim, W., Las Heras, F., Backstein, D., Safir, O., and Pritzker, K.P. Fresh osteochondral allografts for posttraumatic knee defects: long-term followup. *Clin Orthop Relat Res* 466, 1863, 2008.
 14. Emmerson, B.C., Görtz, S., Jamali, A.A., Chung, C., Amiel, D., and Bugbee, W.D. Fresh osteochondral allografting in the treatment of osteochondritis dissecans of the femoral condyle. *Am J Sports Med* 35, 907, 2007.
 15. Jakob, R.P., Franz, T., and Gautier, E. Autologous osteochondral grafting in the knee: indication, results, and reflections. *Clin Orthop Relat Res* 401, 170, 2002.
 16. Temenoff, J.S., and Mikos, A.G. Review: tissue engineering for regeneration of articular cartilage. *Biomaterials* 21, 431, 2000.
 17. Schaefer, D., Martin, I., Jundt, G., Seidel, J., Heberer, M., Grodzinsky, A., Bergin, I., Vunjak-Novakovic, G., and Freed, L.E. Tissue engineered composites for the repair of large osteochondral defects. *Arthritis Rheum* 46, 2524, 2002.
 18. Gun-Il, I., Ji-Hyun, A., So-Young, K., Baek-Sun, C., and Shi-Woo, L. A hyaluronate-atelocollagen/B-tricalcium phosphate-hydroxyapatite biphasic scaffold for the repair of osteochondral defects: a porcine study. *Tissue Eng* 16, 1189, 2010.
 19. Maehara, H., Sotome, S., Yoshii, T., Torigoe, I., Kawasaki, Y., Sugata, Y., Yuasa, M., Hirano, M., Mochizuki, N., Kikuchi, M., Shinomiya, K., and Okawa, A. Repair of large osteochondral defects in rabbits using porous hydroxyapatite/collagen (HAp/Col) and fibroblast growth factor-2 (FGF-2). *J*

Orthop Res 28, 677, 2010.

20. Kon, E., Mutini, A., Arcangeli, E., Delcogliano, M., Filardo, G., Nicoli Aldini, N., Pressato, D., Quarto, R., Zaffagnini, S., and Marcacci, M. Novel nanostructured scaffold for osteochondral regeneration: pilot study in horses. *J Tissue Eng Regen Med* 4, 300, 2010.
21. Oliveira, J.M., Rodrigues, M.T., Silva, S.S., Malafaya, P.B., Gomes, M.E., Viegas, C.A., Dias, I.R., Azevedo, J.T., Mano, J.F., and Reis, R.L. Novel hydroxyapatite/chitosan bilayered scaffold for osteochondral tissue-engineering applications: scaffold design and its performance when seeded with goatbone marrow stromal cells. *Biomaterials* 27, 6123, 2006.
22. Xue, D., Zheng, Q., Zong, C., Li, Q., Li, H., Qian, S., Zhang, B., Yu, L., and Pan, Z. Osteochondral repair using porous poly(lactide-co-glycolide)/nano-hydroxyapatite hybrid scaffolds with undifferentiated mesenchymal stem cells in a rat model. *J Biomed Mater Res A* 94, 259, 2010.
23. Qu, D., Li, J., Li, Y., Khadka, A., Zuo, Y., Wang, H., Liu, Y., and Cheng, L. Ectopic osteochondral formation of biomimetic porous PVA-n-HA/PA6 bilayered scaffold and BMSCs construct in rabbit. *J Biomed Mater Res B Appl Biomater* 96, 9, 2011.
24. Gervaso, F., Scalera, F., Kunjalukkal Padmanabhan, S., Licciulli, A., Deponti, D., Di Giancamillo, A., Domeneghini, C., Peretti, G., and Sannino, A. Development and mechanical characterization of a collagen/hydroxyapatite bilayered scaffold for osteochondral defect replacement. *Key Eng Mater* 493, 890, 2012.
25. Gervaso, F., Scalera, F., Kunjalukkal Padmanabhan, S., Sannino, A., and Licciulli, A. High-performance hydroxyapatite scaffolds for bone tissue engineering applications. *Int J Appl Ceram Technol* 9, 507, 2012.
26. Scalera, F., Gervaso, F., Sanosh, K.P., Sannino, A., and Licciulli, A. Influence of the calcination temperature on morphological and mechanical properties of highly porous hydroxyapatite scaffolds. *Ceram Int* 39, 4839, 2013.
27. Peretti, G.M., Xu, J.W., Bonassar, L.J., Kirchhoff, C.H., Yaremchuk, M.J., and Randolph, M.A. Review of injectable cartilage engineering using fibrin gel in mice and swine models. *Tissue Eng* 12, 1151, 2006.

28. Silverman, R.P., Passaretti, D., Huang, W., Randolph, M.A., and Yaremchuk, M.J. Injectable tissue-engineered cartilage using a fibrin glue polymer. *Plast Reconstr Surg* 103, 1809, 1999.
29. Peretti, G.M., Randolph, M.A., Villa, M.T., Buragas, M.S., and Yaremchuk, M.J. Cell-based tissue engineered allogeneic implant for cartilage repair. *Tissue Eng* 6, 567, 2000.
30. Peretti, G.M., Randolph, M.A., Zaporojan, V., Bonassar, L.J., Xu, J.W., Fellers, J., and Yaremchuk, M.J. A biomechanical analysis of an engineered cell-scaffold implant for cartilage repair. *Ann Plast Surg* 46, 533, 2001.
31. Xu, J.W., Zaporojan, V., Peretti, G.M., Roses, R.E., Morse, K.B., Roy, A.K., Mesa, J.M., Randolph, M.A., Bonassar, L.J., and Yaremchuk, M.J. Injectable tissue-engineered cartilage with different chondrocyte sources. *Plast Reconstr Surg* 113, 1361, 2004.
32. Deponti, D., Di Giancamillo, A., Mangiavini, L., Pozzi, A., Fraschini, G., Sosio, C., Domeneghini, C., and Peretti, G.M. Fibrin-based model for cartilage regeneration: tissue maturation from *in vitro* to *in vivo*. *Tissue Eng Part A* 18, 1109, 2012.
33. Deponti, D., Di Giancamillo, A., Gervaso, F., Domenicucci, M., Domeneghini, C., Sannino, A., and Peretti, G.M. Collagen scaffold for cartilage tissue engineering: the benefit of fibrin glue and the proper culture time in an infant cartilage model. *Tissue Eng Part A* 20, 1113, 2014.
34. Mainil-Varlet, P., Van Damme, B., Nesic, D., Knutsen, G., Kandel, R., and Roberts, S. A new histology scoring system for the assessment of the quality of human cartilage repair: ICRS II. *Am J Sports Med* 38, 880, 2010.
35. Hayes, W.C., Keer, L.M., Hermann, G., and Mockros, L.F. A mathematical analysis for indentation test of articular cartilage. *J Biomech* 5, 541, 1978.
36. Filardo, G., Drobic, M., Perdisa, F., Kon, E., Hribernik, M., and Marcacci, M. Fibrin glue improves osteochondral scaffold fixation: study on the human cadaveric knee exposed to continuous passive motion. *Osteoarthritis Cartilage* 22, 557, 2014.
37. Roche, S., Ronzière, M.C., Herbage, D., and Freyria, A.M. Native and DPPA cross-linked collagen sponges seeded with fetal bovine epiphyseal chondrocytes used for cartilage tissue engineering. *Biomaterials* 22, 9, 2001.
38. Lu, H., Ko, Y.G., Kawazoe, N., and Chen, G. Cartilage tissue engineering using funnel-like

- collagen sponges prepared with embossing ice particulate templates. *Biomaterials* 31, 5825, 2010.
39. Oliveira, S.M., Ringshia, R.A., Legeros, R.Z., Clark, E., Yost, M.J., Terracio, L., and Teixeira, C.C. An improved collagen scaffold for skeletal regeneration. *J Biomed Mater Res A* 94, 371, 2010.
 40. Mizuno, S., Allemann, F., and Glowacki, J. Effects of medium perfusion on matrix production by bovine chondrocytes in three-dimensional collagen sponges. *J Biomed Mater Res* 56, 368, 2001.
 41. Wang, W., Li, B., Li, Y., Jiang, Y., Ouyang, H., and Gao, C. *In vivo* restoration of full-thickness cartilage defects by poly(lactide-co-glycolide) sponges filled with fibrin gel, bone marrow mesenchymal stem cells and DNA complexes. *Biomaterials* 31, 5953, 2010.
 42. Chou, C.H., Cheng, W.T., Kuo, T.F., Sun, J.S., Lin, F.H., and Tsai, J.C. Fibrin glue mixed with gelatin/hyaluronic acid/chondroitin-6-sulfate tri-copolymer for articular cartilage tissue engineering: the results of real-time polymerase chain reaction. *J Biomed Mater Res A* 82, 757, 2007.
 43. Malicev, E., Radosavljevic, D., and Velikonja, N.K. Fibrin glue improved the spatial uniformity and phenotype of human chondrocytes seeded on collagen scaffolds. *Biotechnol Bioeng* 96, 364, 2007.
 44. Martin, I., Miot, S., Barbero, A., Jacob, M., and Wendt, D. Osteochondral tissue engineering. *J Biomech* 40, 750, 2007.
 45. Kon, E., Filardo, G., Di Martino, A., Busacca, M., Moio, A., Perdisa, F., and Marcacci, M. Clinical results and MRI evolution of a nano-composite multilayered biomaterial for osteochondral regeneration at 5 years. *Am J Sports Med* 42, 158, 2014.
 46. Filardo, G., Kon, E., Perdisa, F., Di Matteo, B., Di Martino, A., Iacono, F., Zaffagnini, S., Balboni, F., Vaccari, V., and Marcacci, M. Osteochondral scaffold reconstruction for complex knee lesions: a comparative evaluation. *Knee* 20, 570, 2013.
 47. Sosio, C., Boschetti, F., Bevilacqua, C., Mangiavini, L., Scotti, C., Buragas, M.S., Biressi, S., and Peretti, G.M. Effect of blood on the morphological, biochemical, and biomechanical properties of engineered cartilage. *Knee Surg Sports Traumatol Arthrosc* 15, 1251, 2007.
 48. Sosio, C., Boschetti, F., Mangiavini, L., Scotti, C., Manzotti, S., Buragas, M.S., Biressi, S., Frascini, G., Gigante, A., and Peretti, G.M. Blood exposure has a negative effect on engineered

cartilage. *Knee Surg Sports Traumatol Arthrosc* 19, 1035, 2011.

49. Scotti, C., Osmokrovic, A., Wolf, F., Miot, S., Peretti, G.M., Barbero, A., and Martin, I. Response of human engineered cartilage based on articular or nasal chondrocytes to interleukin-1 β and low oxygen. *Tissue Eng Part A* 18, 362, 2012.
50. Kon, E., Filardo, G., Delcogliano, M., Fini, M., Salamanna, F., Giavaresi, G., Martin, I., and Marcacci, M. Platelet autologous growth factors decrease the osteochondral regeneration capability of a collagen-hydroxyapatite scaffold in a sheep model. *BMC Musculoskelet Disord* 27, 11, 2010.
51. Perdisa, F., Filardo, G., Di Matteo, B., Marcacci, M., and Kon, E. Platelet rich plasma: a valid augmentation for cartilage scaffolds? A systematic review. *Histol Histopathol* 29, 805, 2014.
52. Roffi, A., Filardo, G., Kon, E., and Marcacci, M. Does PRP enhance bone integration with grafts, graft substitutes, or implants? A systematic review. *BMC Musculoskelet Disord* 21, 330, 2013.
53. Betsch, M., Schnependahl, J., Thuns, S., Herten, M., Sager, M., Jungbluth, P., Hakimi, M., and Wild, M. Bone marrow aspiration concentrate and platelet rich plasma for osteochondral repair in a porcine osteochondral defect model. *PLoS One* 8, e71602, 2013.
54. Filová, E., Rampichová, M., Litvinec, A., Držík, M., Míčková, A., Buzgo, M., Košťáková, E., Martinová, L., Usvald, D., Prosecká, E., Uhlík, J., Motlík, J., Vajner, L., and Amler, E. A cell-free nanofiber composite scaffold regenerated osteochondral defects in miniature pigs. *Int J Pharm* 447, 139, 2013.
55. Deponti, D., Di Giancamillo, A., Scotti, C., Peretti, G.M., and Martin, I. Animal models for meniscus repair and regeneration. *J Tissue Eng Regen Med* 2013 [Epub ahead of print]; DOI: 10.1002/term.1760.
56. Proffen, B.L., McElfresh, M., Fleming, B.C., and Murray, M.M. A comparative anatomical study of the human knee and six animal species. *Knee* 19, 493, 2012.

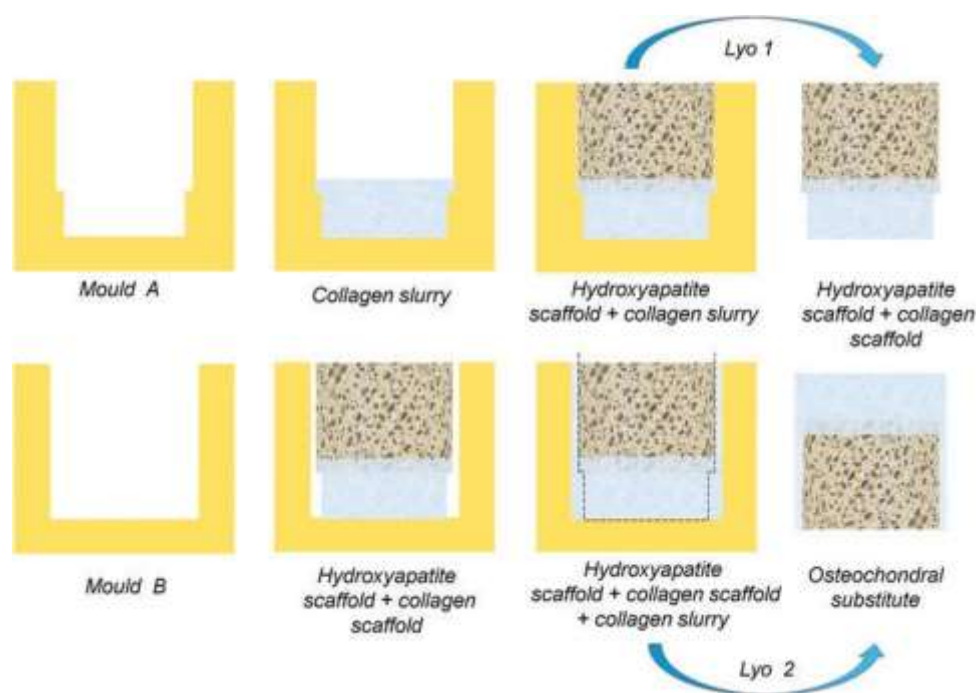


FIG. 1. A schematic representation of the procedure for the bilayered substitute fabrication (see Material andMethods section).

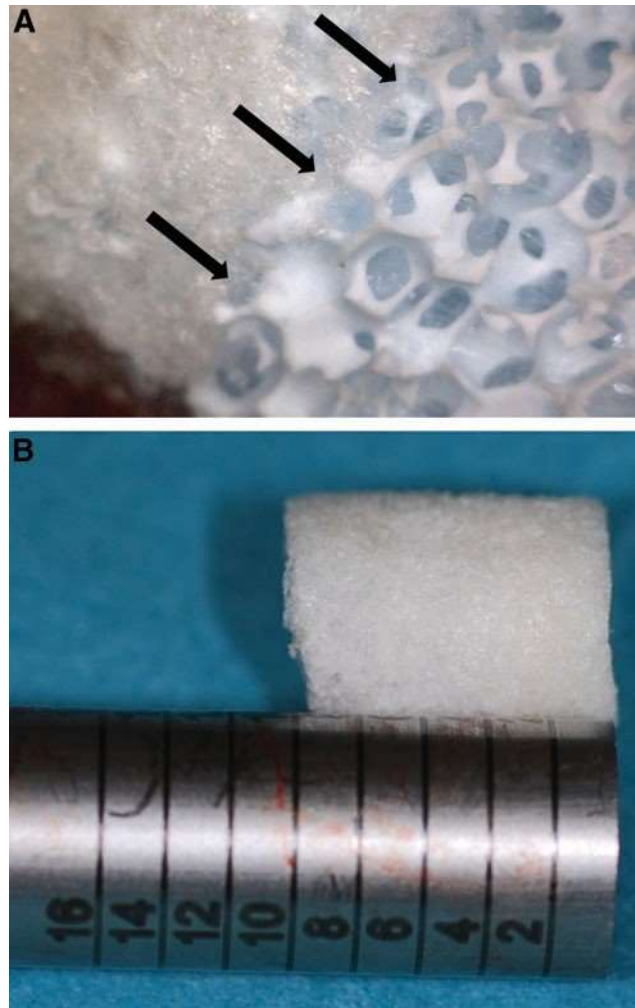


FIG. 2. Characteristics of the bilayered scaffold. (A) Detail of the integration between the collagen and the hydroxyapatite layers (black arrows). (B) A scaffold at the end of the fabrication process surrounded by a thin layer of collagen, together with the core punch utilized in the animal surgery.

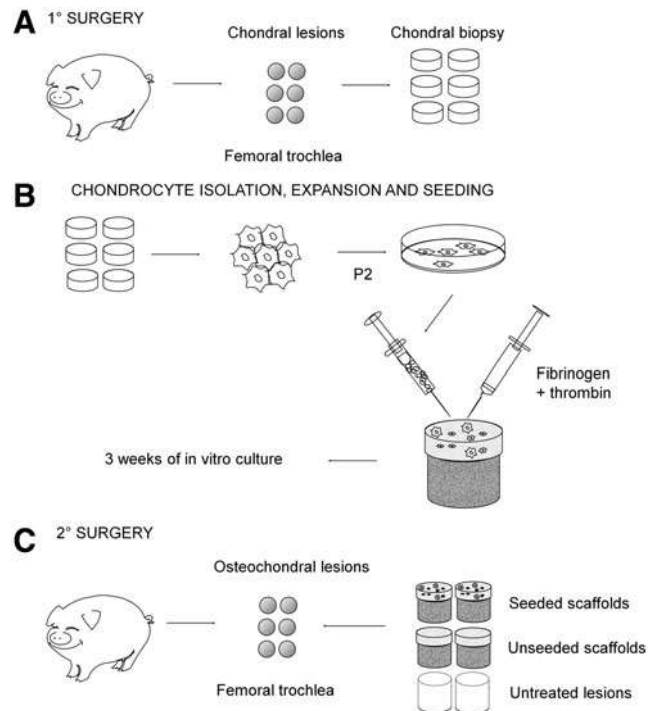


FIG 3 (A) Six chondral lesions were done in the right trochlea of six pigs. (B) The six chondral biopsies were digested and the autologous chondrocytes were isolated; then the cells were expanded in culture and finally seeded in the chondral portion of the scaffold; the seeded scaffolds were cultured in chondrogenic medium for 3 weeks and then implanted. (C) With a second surgery, the repairing tissue formed in the chondral lesions was removed generating six osteochondral lesions; in each animal, two lesions were implanted with seeded scaffold, two lesions with unseeded scaffolds, while the remaining two lesions were left untreated.

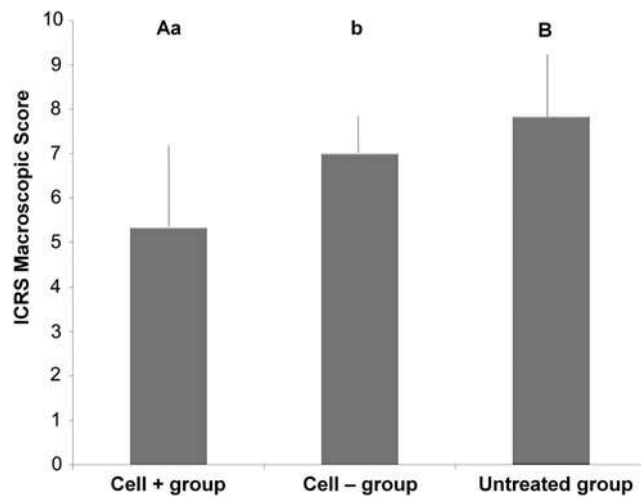


FIG. 4. International Cartilage Repair Society (ICRS) macroscopic score comparison between the groups. Values with different superscripts differ for $p < 0.01$ (A,B) and $p < 0.05$ (a,b). The score employed here (y-axis) ranges from 0 to 10.

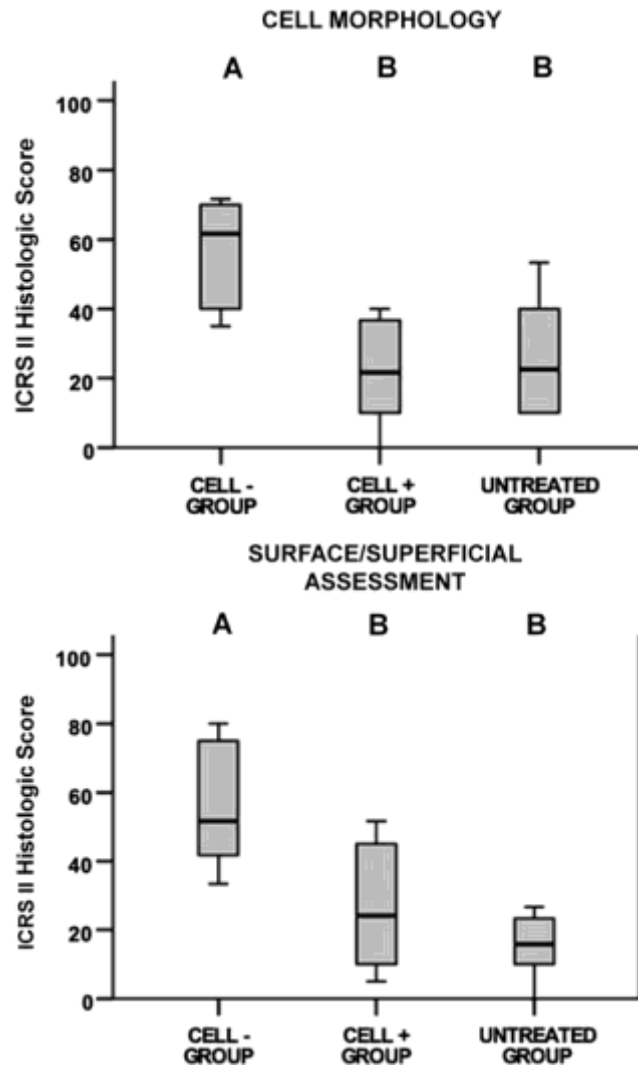


FIG 5. ICRS II visual histological score comparison between the groups. Only the two parameters (cell morphology and surface/superficial assessment) that have shown statistically significant differences are reported. Values with different superscripts differ for $p < 0.01$ (A,B). The score employed here (y-axis) ranges from 0 to 100.

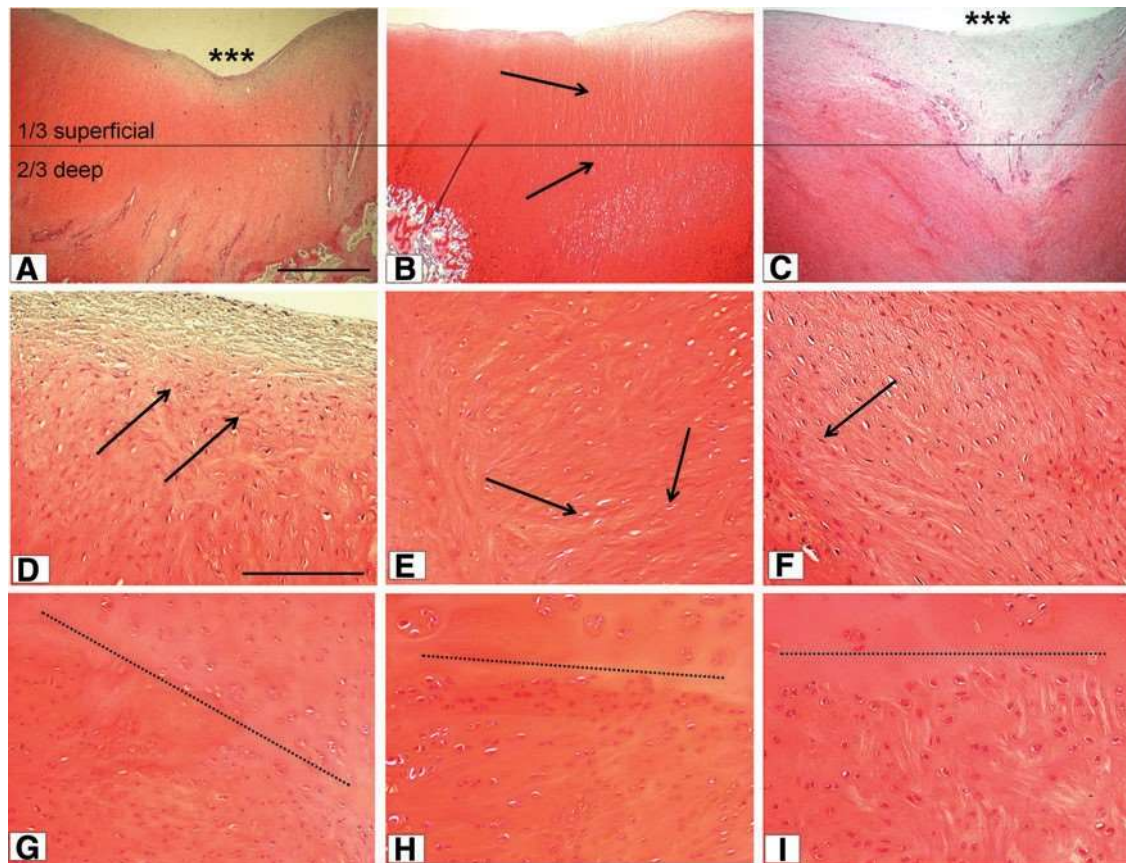


FIG. 6. Histological findings of the repaired tissue after 3 months (Safranin O staining). Evaluation of the surface/ superficial assessment (A–C), performed on the upper third of the cartilage tissue, and cell morphology (D–F, arrows). Integration of the reparative tissue with the native cartilage (G–I, dotted lines). (A, D, G) Untreated group; (B, E, H) cell - group; (C, F, I) cell + group. Scale bar: (A–C) 500 mm; (D–I) 200 mm. Asterisks highlight the superficial depression areas.

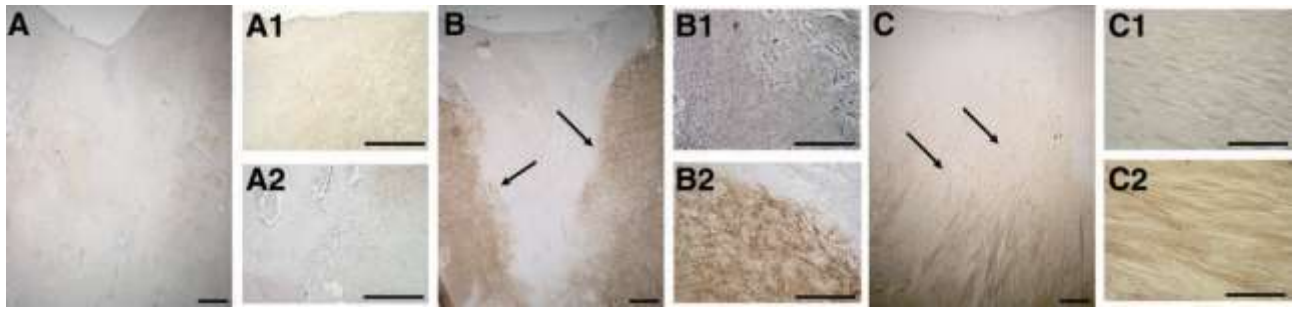


FIG. 7. Immunohistochemistry of the repaired tissue for type II collagen. (A) Untreated group; (B) cell - group; (C) cell + group. For every group, one detail of the superficial level (A1–C1) and one of the deep level (A2–C2) were reported. The arrows in (B and C) show the areas positive to type II collagen. Scale bar: 200 mm (see Result section for explanation).

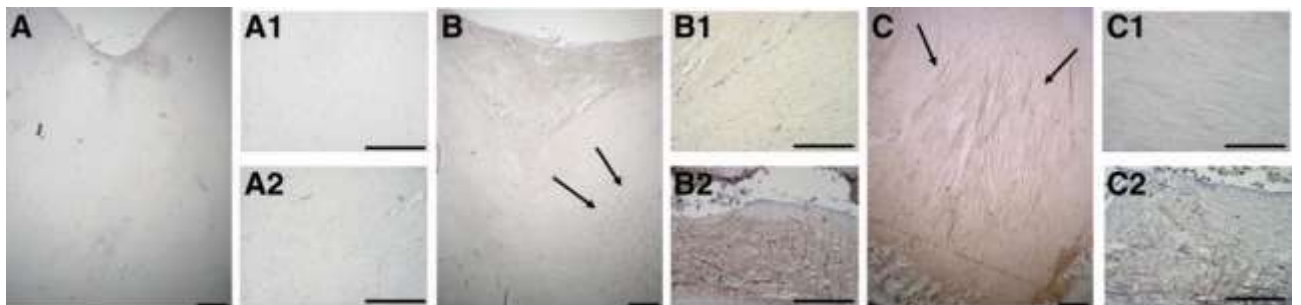


FIG. 8. Immunohistochemistry of the repaired tissue for type I collagen. (A) Untreated group; (B) cell - group; (C) cell + group. For every group, one detail of the superficial level (A1–C1) and one of the deep level (A2–C2) were reported. The arrows in (B and C) show the areas positive to type I collagen. Scale bar: 200 mm (see Result section for explanation).

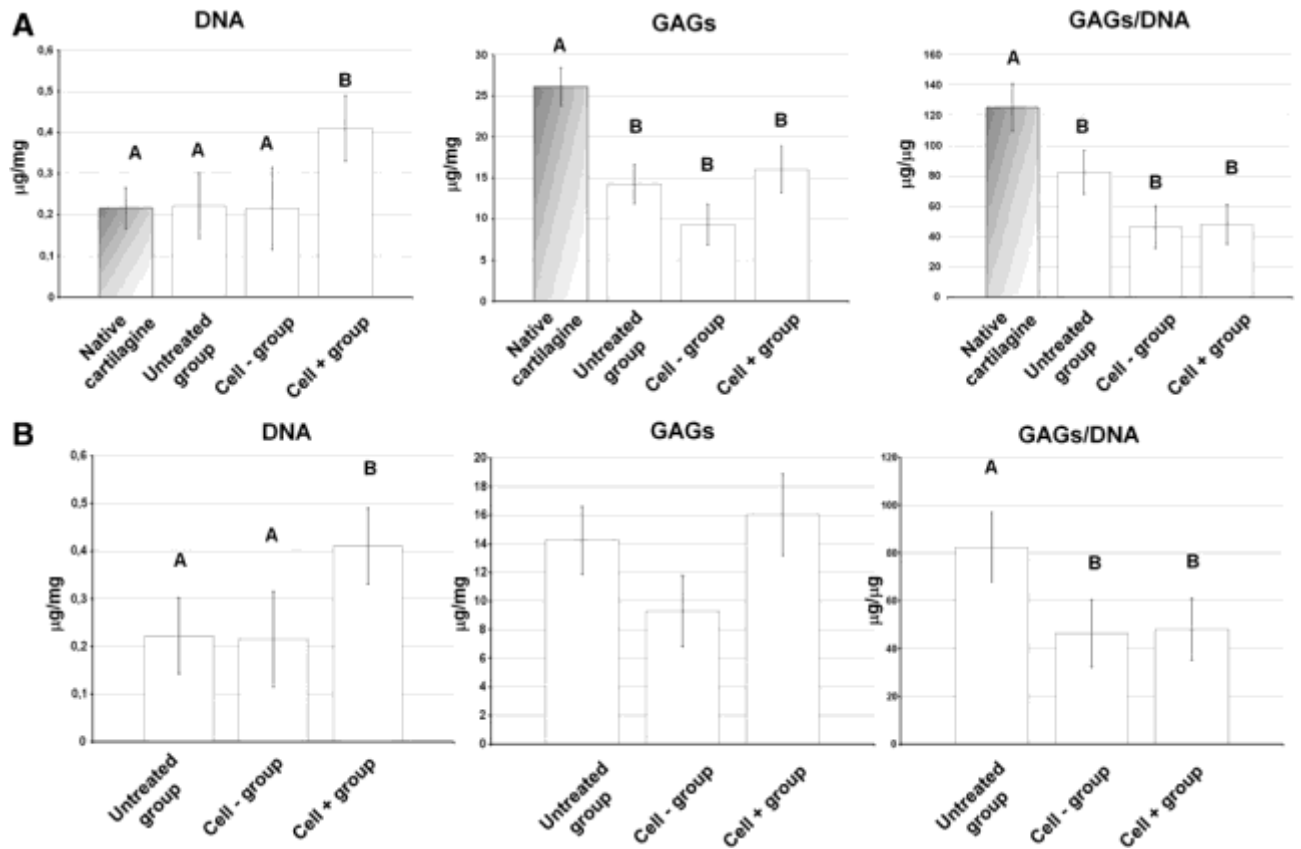


FIG. 9. Biochemical analysis of the repaired tissue: DNA quantification as index of cellularity (mg/mg wet weight); glycosaminoglycans (GAG) quantification (mg/mg wet weight); GAG/DNA ratio (mg/mg). (A) Biochemical analysis of the experimental samples with respect to the native cartilage. (B) Biochemical analysis of the experimental samples with respect to the different treatments. Values with different superscripts differ for $p < 0.01$ (A,B).

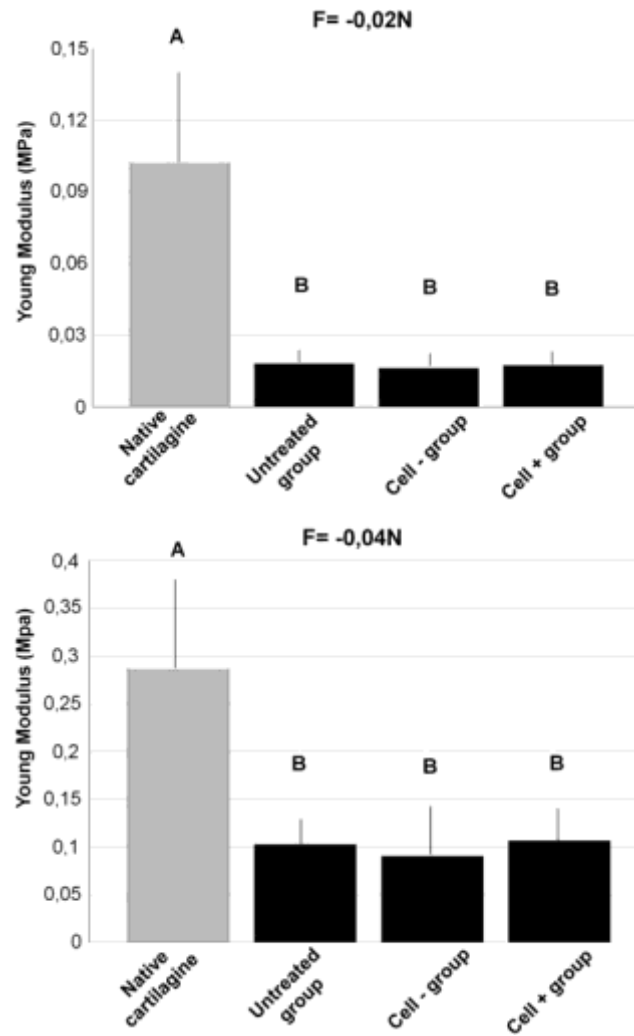


FIG 10. Biomechanical analysis of the repaired tissue from indentation test. Biomechanical analysis of the experimental samples with respect to the native cartilage applying two increasing levels of force (-0.02 and -0.04 N). Values with different superscripts differ for $p < 0.01$ (A,B).